

Construction And Operation Of The Eindhoven MHD Blow-Down Facility

Author(s): W. J. M. Balemans, P. Masee, and L. H. Th. Rietjens

Session Name: Status Reports National Programs, Part B

SEAM: 26 (1988)

SEAM EDX URL: <https://edx.netl.doe.gov/dataset/seam-26>

EDX Paper ID: 1248

CONSTRUCTION AND OPERATION OF THE EINDHOVEN MHD BLOW-DOWN FACILITY

W.J.M. Balemans, P. Massee and L.H.Th. Rietjens

Eindhoven University of Technology
Group Electrical Energy Systems
Eindhoven, The Netherlands

ABSTRACT

In this paper the experiences with the Eindhoven MHD blow-down facility are described. The attention is focussed especially on the construction of the generator channel, on the conditions necessary for optimum MHD operation and on the obtained results. The static pressure distributions indicate that the maximum enthalpy extraction (12.9%) has been obtained in the present hot flow train. For a further increase of the enthalpy extraction a modification of the hot flow train would be necessary.

INTRODUCTION

Figure 1 shows a line diagram of the Eindhoven MHD blow-down facility. Details of the operation of the facility have been presented in previous papers^{1,2,3}. With this facility eight measurement series have been carried out. In early experiments not more than four power runs could be performed consecutively and the measurement series had to be terminated because of mechanical failure of the generator channel⁴. Analysis of the structural problems and modification of the channel construction made it possible to perform 22 power runs in measurement series 8. Also important in this connection was the fact that the supersonic diffuser which is partly situated within the magnetic field was changed from a stainless steel to an isolating wall construction. The experience with the mentioned constructions and with the operation of the facility is described in the next section. Further some results of the experiments will be presented. Results from special diagnostic techniques are presented in a separate paper at this conference⁵.

CONSTRUCTION AND OPERATION

The aerodynamic shape of the generator channels of the Eindhoven MHD blow-down facility have been determined by means of a quasi-one-dimensional generator model for operation in the segmented Faraday mode. This model does not include the ionization relaxation process. The predictions of the model hold if the relaxation length is small with respect to the length of the generator. This condition can be met at sufficiently high values of the magnetic induction or by appropriate pre-ionization.

One of the special constraints that the blow-down facility requires is that it has to exhaust into the

ambient atmosphere. The mechanical design was made for operation in the heat-sink mode. In the blow-down facility, generator channels are at room temperature just before the run starts. Due to the hot test gas (stagnation temperature 1900 K) the inner walls of the generator duct will be heated up suddenly. Therefore it is necessary that the applied inner wall material has a good thermal shock resistance. Also the material may not be attacked by the cesium in the test gas, meaning that a possible reaction of the material with cesium may not form an electrically conducting layer which could lead to short circuiting in the generator. Candidate materials for the inner wall of the generator channel are boron nitride and silicon nitride.

In a Faraday loaded MHD generator under operation conditions there is also an electric field in the axial direction in the order of 1000 V/m, the so called Hall-field. To prevent possible short circuiting the outer shell of the generator is made of glass fibre reinforced epoxy resin, and all the downstream components are electrically insulated from ground. The maximum operating temperature of the epoxy is 400 K while the inner wall material can reach temperatures up to 1200 K. So a good thermal insulator is necessary between the inner wall and the outer shell and additional cooling of the epoxy after the run is required.

During the eight series of measurements five different generator channels have been used all with an inlet Mach number of 1.66. In principle the construction of the channels has not changed very much. The main differences between the last and the first channel are a simplification of the form of the inner wall plates to prevent stress concentrations due to notches and the use of ceramic bonding between inner wall plates and insulation plates to prevent a gas flow in between. Table I shows the design characteristics of the different channels. All channels have the same inlet and outlet cross section because always the same nozzle and diffuser system have been used (the outlet cross section is limited by the warm bore in the magnet). Therefore a change in divergence of the channel implies a change of the length. Figure 2 gives an impression of the construction of the channel used in series 7 and 8.

In the measurement series 2 to 6 the planned experimental program has always been interrupted due to mechanical problems with the generator channel. Analysis of the results learned that in the downstream part of the generator and in the diffuser system large

pressure fluctuations of about 1 bar at frequencies of 1 kHz occurred. This is caused by an instationary power extraction process when the MHD conditions are not optimal. These fluctuations resulted in high mechanical stresses which combined with the present thermal stresses led to fracture of the ceramic material. During the power runs of series 2 to 6 there was a large discrepancy between the measured static pressure distribution and the theoretically calculated values (see figure 15). This was caused by the fact that the supersonic part of the diffuser, which was constructed of stainless steel, was partly located in a high magnetic field. Figure 3 shows the value of the maximum magnetic induction in generator and diffuser. Consequently the supersonic part of the diffuser worked as a generator, short circuited in both Faraday and Hall direction. Therefore the interaction on the test gas was so high that the velocity decreased substantially and consequently the pressure increased strongly. In series 7 the stainless steel supersonic diffuser was partly replaced by an electrically insulated one and after run 810 this insulated part was enlarged with 0.216 m to decrease the maximum magnetic induction in the stainless steel part from 50% to 20% of the effective magnetic induction. Together with the replacement of load resistors which had a rather high self inductance (525 μH) by load resistors having a fairly low self inductance (1.15 μH) and an improvement of the cesium injection, this has led to a situation without large pressure fluctuations in the generator channel and without the resulting mechanical problems.

As mentioned above the stainless steel supersonic diffuser has been partly replaced by an electrically insulated one after series 6. Figure 4 shows the construction of the insulated part of the supersonic diffuser. The inner wall is built up from small boron nitride tiles which are interlocked with the surrounding tiles by means of grooves and are individually fixed with a stainless steel bolt on insulated copper cooling panels. The small boron nitride tiles are provided with screw-thread in which a helicoil is placed. This construction is suitable for the purpose and is easy to make. To prevent short circuiting, the copper cooling panels have ceramic inserts and an araldite coating which is tested up to 2000 V. The araldite coating is maintained at temperatures below 400 K by cooling the copper plates with water and by using an alumina fibre material between the boron nitride tiles and the coating. The coated copper cooling panels are surrounded by a gas-tight glass fibre reinforced epoxy resin shell.

After measurement series 2 to 6 it has been concluded that proper MHD results cannot be obtained during the first power run after the installation has been exposed to air. In such circumstances the level of molecular contaminants is generally very high due to outgassing of the channel walls. Figures 5 and 6 show that the contamination levels drop considerably from the first to the second run.

POWER EXTRACTION RESULTS

The most important parameters of various runs are shown in the tables II to IV. The experimental results have been obtained in 8 measurement series and include a total of about 50 runs. Rather than presenting the parameters of all runs in one large table the results are separated in three smaller tables at a (more or

less) constant value of the load resistance for ease of comparison. Measurement series 1 was used for thermal and mechanical tests of the facility before the magnet was installed. In measurement series 2 and 3 a maximum electrical power output of 362 kW (enthalpy extraction = 7.2%) was produced in run 303 (see table II). In measurement series 4, 5 and 6 very low power outputs (from less than 1 kW up to 60 kW) were produced at the same loading conditions of the generator as in run 303. This can be explained by the very high level of molecular contaminants which was present during the power runs of measurement series 4 and by the influence of the large self induction of the loads. After analysis of the problems and small modifications of the installation significant enthalpy extraction was again obtained in measurement series 7 and 8. A maximum power output of 735 kW was obtained in run 808 which is illustrated in figure 7 together with the magnetic induction as a function of time. The largest number of runs (a total of 25) was produced in measurement series 8 since the channel life no longer dictated the maximum experimental operating time. Due to this the influence of the variation of parameters on the electrical power output could be investigated extensively in this measurement series. Over all the experiments performed up to now the percentage of cesium seeding has been varied from 0.01 up to 0.2, the load resistance from 2.7 up to 9 Ohm and the stagnation pressure from 6 up to 8.7 bar. A variation of stagnation temperature has also been attempted but was difficult to obtain. Besides that the influence of the variation of segmentation length has been studied during runs 704 and 705. During these runs only the odd numbered electrodes were at first connected to 3.65 Ohm resistors. At the time of maximum magnetic induction this situation was switched to the condition in which all electrode pairs were connected to 7.3 Ohm resistors. This change results in the same loading condition of the channel but the segmentation length is halved (from 5.6 to 2.8 cm). The change in electrical power output was hardly noticeable.

The best insight in the influence of the variation of cesium seeding on the power output has been obtained during the runs 703 and 802. In these runs the cesium flow was varied about a factor 2 (see table II) during 10 s around the condition of maximum magnetic induction so that the strength of the magnetic field varies only 10% (compare figure 7 for run 808). The interpretation of the results is not easy due to the hysteresis effect shown in figure 8 for run 808 but no significant influence of the seeding on the power output could be established. In order to limit problems due to accumulation of cesium the seeding percentage was further chosen on the low side of the range investigated. The lowest value of cesium seeding of 0.01% during run 818 only resulted in a higher total Hall potential (1300 V which is about 2 times the normal value) but not in a larger power output (see table III).

The influence of the variation of stagnation pressure on the maximum enthalpy extraction is plotted in figure 9. These results were obtained from runs 803, 804, 807, 808 and 809 which were all performed with a load resistance of 3.6 Ohm (see table III). Since the maximum magnetic induction was limited to 4.3 T during run 804 the results plotted in figure 9 are taken at this common value of the magnetic induction. Due to the hysteresis effect shown in figure 8 there are in

general two different values of enthalpy extraction at 4.3 T. For figure 9 the value of enthalpy extraction at 4.3 T is taken at a time during the run larger than the time of maximum magnetic induction (compare figure 7). As can be seen from table III there is a small variation in stagnation temperature and in cesium seeding during the runs used for figure 9. During the runs 803 and 809 which were both performed at 7 bar, the stagnation temperature differed 40 K. The resulting change in enthalpy extraction at a value of 4.3 T equals one percentage point. Figure 9 indicates that the enthalpy extraction reaches a maximum at a stagnation pressure between 7 and 8 bar. It should be mentioned that the runs from 811 to 825 have not been used for figure 9. The good reproducibility of results obtained during the runs 801 to 810 (especially runs 803 and 809) could not be duplicated during the runs from 811 to 825. In general the enthalpy extraction obtained during the runs 811 to 825 is considerably less than the value for a run with comparable parameters in the series from 801 to 810. Table III shows that the runs 817 and 823 seem to form a favourable exception to this rule. An explanation of these discrepancies has not yet been identified.

The influence of a variation of load resistance on the enthalpy extraction is shown in figure 10 for a stagnation pressure of 7 bar. These results were obtained from runs 802, 803, 805, 809 and 810; the plotted data were taken at values of the magnetic induction of 4.3, 4.8 and 5.0 T. The data in figure 10 indicate that the maximum enthalpy extraction is obtained at a value of the load resistance between 2.7 and 3.6 Ohm. An interesting point to note is the large difference at a load resistance of 5.4 Ohm between the enthalpy extraction at magnetic inductions of 4.3 and 4.8 T. This is probably caused by the observed increase of water contamination during run 802 (the first power run after the channel has been exposed to the air).

As has been mentioned before the maximum enthalpy extraction of measurement series 2 and 3 has been limited to 7.2% whereas in later measurement series the enthalpy extraction could be increased to 12.9%. An illustration of different behaviour of the MHD generator during measurement series 3 as compared to measurement series 8 is shown in the current distributions in figure 11. It is seen that the current is about constant after the relaxation region in run 803 but the current decreases strongly in the second half of the generator during run 302. Combined with the behaviour of the current of electrodepairs in the second half of the generator as a function of time this suggested Hall shorting problems during run 302. Figure 12, however, shows that this is not supported by the measured Hall voltage distribution which is positive for all values of x during both run 302 and run 803. The negative values of the Hall voltage in the inlet region of the generator as shown for run 703 are explained by a partial Hall shorting to ground at the last observation window (near electrode 25). Another illustration of different behaviour of the MHD generator during measurement series 3 and 8 can be obtained by comparing the static pressure distributions given in the figures 13 and 14. The strong increase of static pressure in the second half of the generator during measurement series 3 could not be explained by quasi-one-dimensional flow calculations even when the displacement thicknesses of the MHD boundary layers were taken into account⁶. (see figure 13).

After modification of the first part of the supersonic diffuser into a construction with insulating walls the power output increased significantly and the pressure distribution in the MHD generator also changed strongly. The latter fact is clearly illustrated in figure 14 in which it is very noticeable that the pressure at the generator exit is much lower in the runs 803 and 805 than in run 302 although the enthalpy extraction is a factor 2.8 larger. The static pressure profiles measured during the runs of series 7 and 8 are in agreement with quasi-one-dimensional flow calculations.

Figure 14 shows also very strikingly that the pressure at the exit of the generator increases gradually with increasing enthalpy extraction during measurement series 8. From observation of figure 10 and from tables III and IV it is clear that a decrease of the load resistance from 3.6 to 2.7 Ohm did not lead to an increase of output power. In general the opposite effect would be expected unless boundary layer problems would have been encountered somewhere in the hot flow train. Figure 14 confirms this assumption although the pressure distribution in the generator does not show a significant difference between curves 3 and 4. The pressure distribution in the supersonic diffuser, however, changes significantly when the value of the load resistance is decreased from 3.6 to 2.7 Ohm. A similar phenomenon is observed when the gasdynamic flow is started up by increasing the stagnation pressure up to its steady state value ($t \sim 15s$). Also under those circumstances it is observed that the first indication that the flow is not supersonic throughout the entire generator and the entire supersonic diffuser, is a pressure increase at the downstream side of the latter component. It is therefore concluded from the pressure distributions in figure 14 that a load resistance of 2.7 Ohm implies too much MHD interaction for the present hot flow train at a stagnation pressure of 7 bar. Maximum output power will thus be obtained at a value of the load resistance between 2.7 and 3.6 Ohm; the optimum value will probably be closer to 3.6 than to 2.7 Ohm.

CONCLUSIONS

During the course of the experiments it was discovered that additional requirements have to be fulfilled in order to guarantee optimum MHD conditions in a closed cycle blow-down facility. These requirements are the following:

- when the seed is injected in the form of a spray of small liquid droplets attention must be paid to provide a homogeneous distribution over the cross section.
- the molecular contamination of the generator medium (especially the water contamination) should be below 100 ppm; this can be reached by using the first one or two runs of each measurement series for outgassing of the generator walls.
- components of the hot flow train inside the magnetic field should not contain metal walls in contact with the plasma in order to prevent short circuiting of internal electric currents.
- the external loads should not have a large self inductance because this will prevent the creation of a sufficient number of streamers.

When optimum MHD conditions and thus a sufficient number of streamers are present, the power extraction process and thus the static pressures do not show

fluctuations on a time scale of the characteristic flow time. Under those circumstances the thermal and mechanical problems of a heat sink channel have been solved so that many runs could be obtained within one measurement series.

The experimental data obtained in measurement series 7 and 8 give the possibility to improve the modelling of closed cycle MHD generators. This is part of the present research program of our group and is reported in a separate paper at this symposium⁷.

ACKNOWLEDGEMENT

This work was performed with financial support from the Netherlands Technology Foundation (STW).

REFERENCES

1. Blom, J.H. et al., "Design of the Eindhoven 5 MW Thermal MHD Blow-down Experiment", 17th Symp. on Eng. Asp. of MHD, p. H4.1., Stanford, Cal., 1978.
2. Blom, J.H. et al., "First Experiments with the Eindhoven 5 MW Thermal MHD Blow-down Experiment", VIIth Int. Conf. on MHD Electrical Power Generation, Vol. I, p. 102., Cambridge, Mass., 1980.
3. Balemans, W.J.M. and Rietjens, L.H.Th., "High Enthalpy Extraction Experiments with the Eindhoven Blow-down Facility", Proc. 9th Int. Conf. on MHD Electrical Power Generation, Vol. II, p. 330, Tsukuba, 1986.
4. Flinsenberg, H.J., Balemans, W.J.M. and Rietjens, L.H.Th., "Power Extraction Experiments with the Eindhoven Blow-down Facility", Proc. VIIIth Int. Conf. on MHD Electrical Power Generation, Vol. I, p. 80, Moscow, 1983.
5. van Veldhuizen, E.M., "An Overview of Diagnostic Results of the EUT Blow-down Generator", 26th Symp. on Eng. Asp. of MHD, Session 9, Nashville, 1988.
6. Masee, P., "Gasdynamic Performance in Relation to the Power Extraction of an MHD Generator", Ph.D. thesis, EUT, Eindhoven, 1983.
7. Merck, W.F.H., Masee, P. and Rietjens, L.H.Th., "An Empirical Approach to the Electrical Performance of a Closed Cycle MHD Generator", 26th Symp. on Eng. Asp. of MHD, session 9, Nashville, 1988.

Table I. Characteristic data of the generator channels.

Channel number	1	2	3	4	5
series of measurement	1+2	3	4+5	6	7+8
material inner wall	BN	Si ₃ N ₄	BN	BN	Si ₃ N ₄
material insulation	porous alumina	porous alumina	alumina fibre	alumina fibre	alumina fibre
material outer shell	epoxy resin	epoxy resin	epoxy resin	epoxy resin	epoxy resin
material electrodes	stainless steel	stainless steel	molybdenum	stainless steel	stainless steel
number of electrodes	32	32	32	25	25
width electrodes (mm)	4	4	7	8	8
pitch electrodes (mm)	25	25	25	28	28
inlet area (mm ²)	50x150	50x150	50x150	50x150	50x150
outlet area (mm ²)	180x150	180x150	180x150	180x150	180x150
length (mm)	800	800	800	700	700
window pairs (number)	2	2	1	3	3
pressure probes (number)	5	5	4	16	14
voltage probes (number)	3x5	3x5	3x5	4x12	4x12
thermocouples (number)	27	27	21	19	19

Table II. Parameters of various runs at a load resistance of about 6 Ohm.

Run	T _s (K)	p _s (bar)	B (T)	R _L (Ω)	Cs (%)	P _{e max} (kW)	η _{ent} (%)	H ₂ O (ppm)	N ₂ (ppm)	CO ₂ (ppm)
204	1870	7.2	5.3	6	0.04	270	5.6	60	25	
303	1900	7.4	5.1	6	0.14	362	7.2	50	200	
702	1920	7.2	5.2	5.6	0.11	393	7.9	150	100	< 20
703	1910	7.2	5.1	5.6	0.11- 0.20	413	8.5	125	100	< 20
802	1920	7.0	4.8	5.4	0.06- 0.15	404	8.4	2500 ^{a)}	< 50	250 ^{a)}

Explanation of the symbols

T_s: stagnation temperature
 p_s: stagnation pressure
 B: magnetic induction
 R_L: load resistance
 Cs: molecular fraction of cesium
 P_e: electrical power output
 η_{ent}: enthalpy extraction
 H₂O: water contamination level
 N₂: nitrogen contamination level
 CO₂: carbon dioxide contamination level

a) measurement strongly influenced by impurities in the detection system.

Table III. Parameters of various runs at a load resistance of about 4 Ohm (and at low contamination levels).

Run	T _s (K)	p _s (bar)	B (T)	R _L (Ω)	Cs (%)	P _{e max} (kW)	η _{ent} (%)	H ₂ O (ppm)	N ₂ (ppm)	CO ₂ (ppm)
205	1910	7.2	5.3	4	0.05	286	5.8	60	60	
803	1940	7.0	5.2	3.6	0.075	621	12.9	< 100	< 50	150
804	1930	6.0	4.3	3.6	0.08	424	10.2	100	< 50	< 20
807	1920	8.0	5.2	3.6	0.06	667	12.2	400	< 50	< 20
808	1910	8.7	5.5	3.6	0.10	735	12.3	< 100	< 50	< 20
809	1900	7.0	5.0	3.6	0.07	530	11.0	< 100	< 50	< 20
817	1920	7.3	5.3	3.6	0.09	538	10.8			
818	1920	7.3	5.5	3.6	0.01	392	7.8	< 60	< 40	< 40
821	1890	8.1	5.2	3.6	0.07	320	5.8	60	60	< 20
822	1910	8.2	5.6	3.6	0.06	401	7.1	< 40	50	< 20
823	1890	7.3	5.4	3.6	0.07	489	9.8	< 40	< 20	< 20

Table IV. Parameters of various runs at a load resistance of 2.7 Ohm.

Run	T _s (K)	p _s (bar)	B (T)	Cs (%)	P _{e max} (kW)	η _{ent} (%)	H ₂ O (ppm)	N ₂ (ppm)	CO ₂ (ppm)
805	1930	7.1	5.0	0.06	591	12.1	< 100	< 50	< 20
806	1940	8.0	5.0	0.055	652	11.8	250	< 50	< 20
819	1900	7.3	5.0	0.075	304	6.1	< 60	< 40	< 40

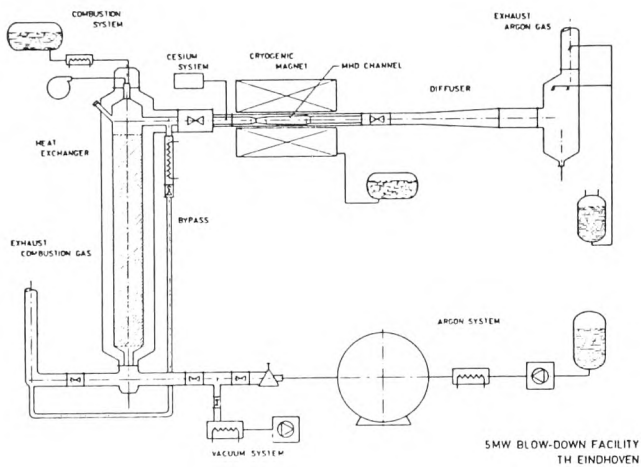


Fig. 1 Line diagram of the MHD blow-down facility.

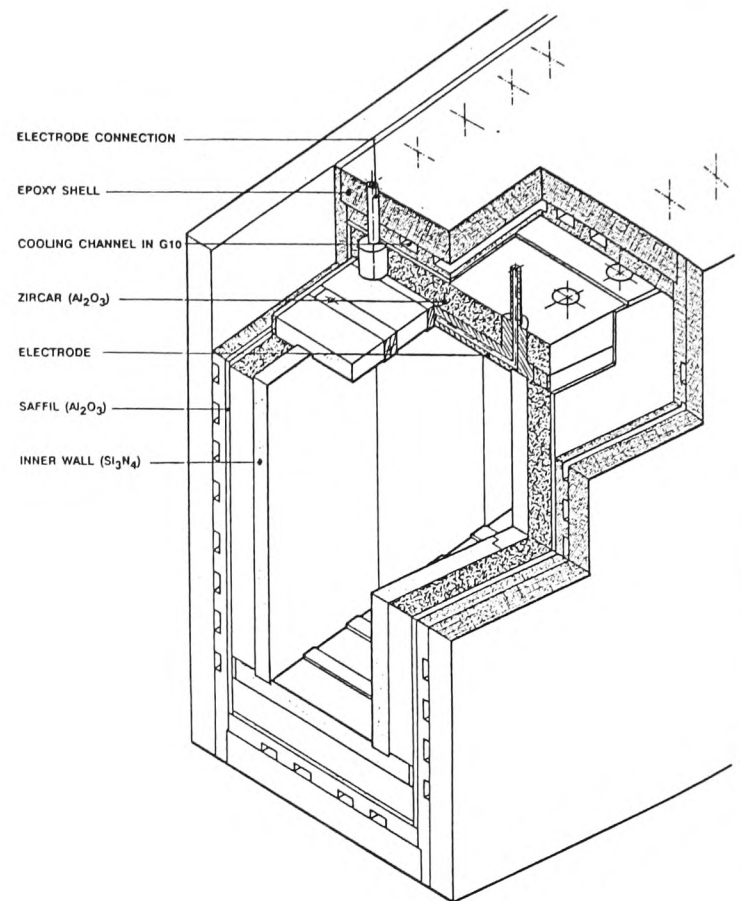


Fig. 2 Construction of the generator channel.

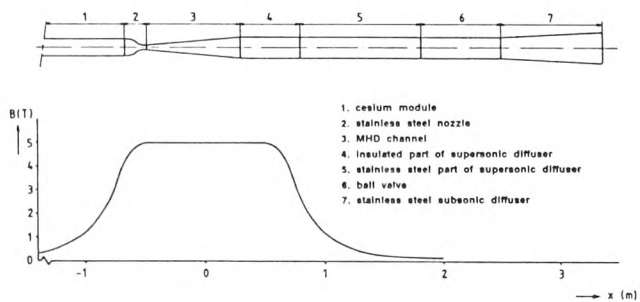


Fig. 3 Magnetic induction (B) as a function of the distance in the hot flow-train.

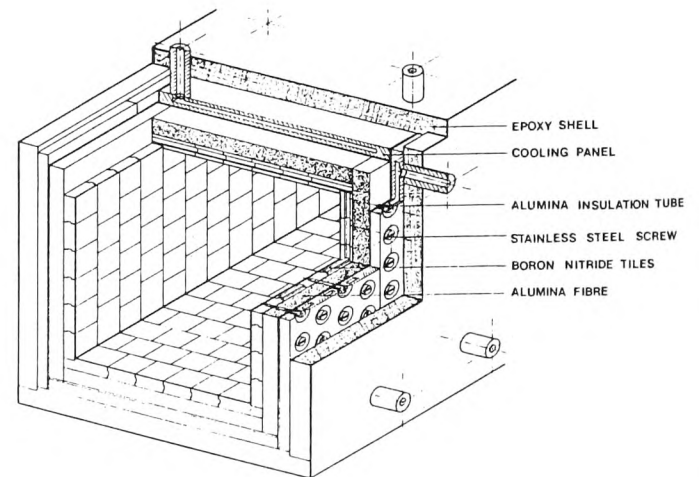


Fig. 4 Construction of the supersonic diffuser.

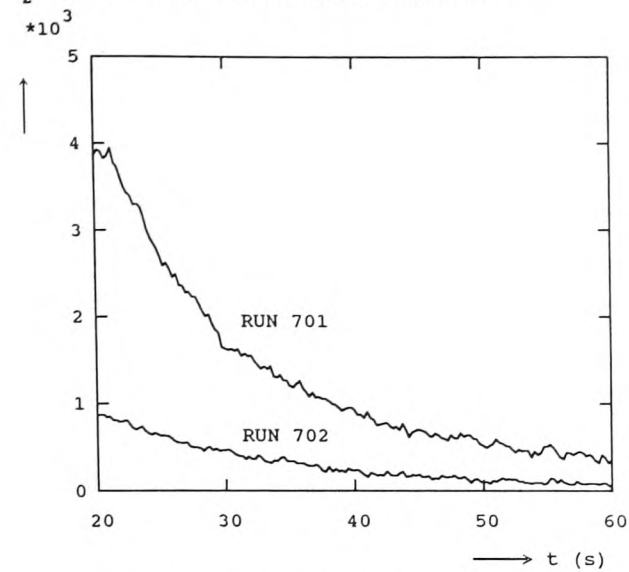
H_2O (ppm) mass spectrometer measurement

Fig. 5 Molecular impurity level of H_2O during runs 701 and 702. The power extraction of run 702 is from 40 to 60 s.

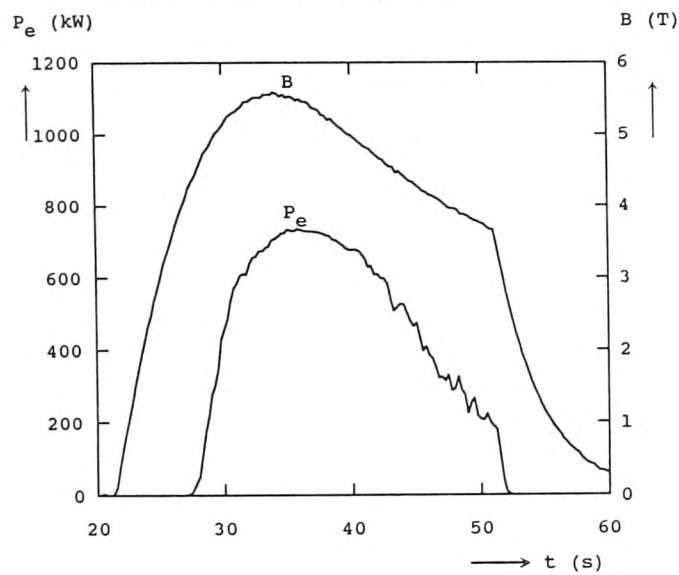


Fig. 7 Electrical power output (P_e) and magnetic induction (B) during run 808.

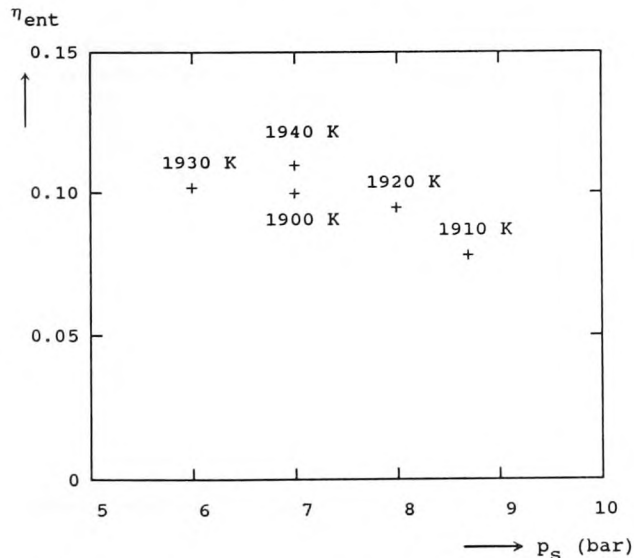


Fig. 9 Enthalpy extraction (η_{ent}) as a function of stagnation pressure (p_s) at $B = 4.3$ T and $R_L = 3.6$ ohm.

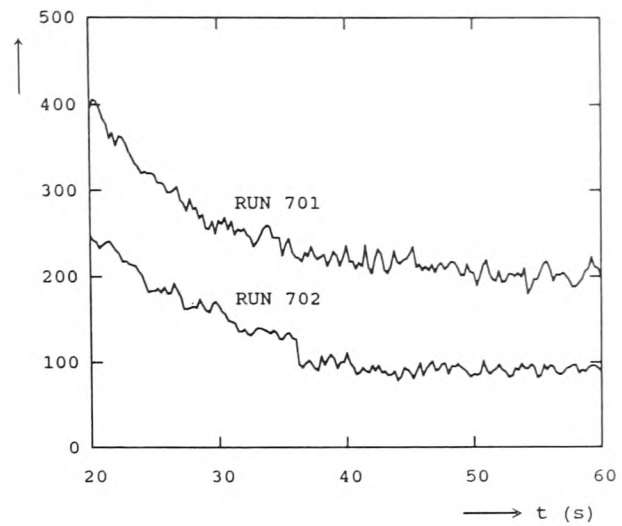
 N_2 (ppm) mass spectrometer measurement

Fig. 6 Molecular impurity level of N_2 during runs 701 and 702. The power extraction of run 702 is from 40 to 60 s.

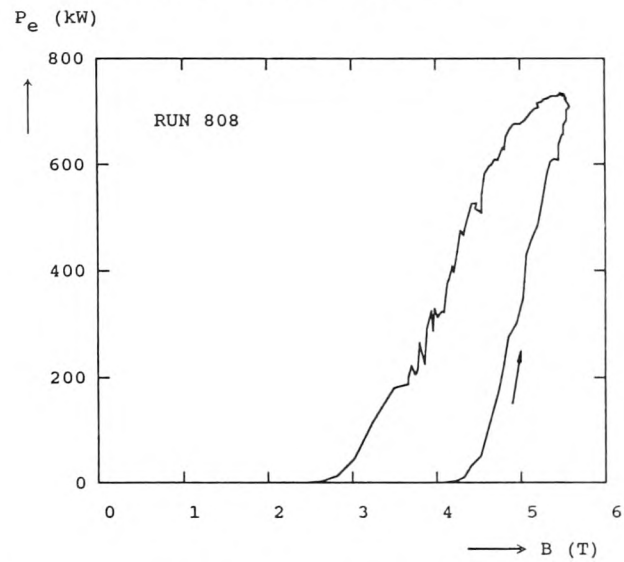


Fig. 8 Electrical power output (P_e) as a function of magnetic induction (B) during run 808. Note that the arrow indicates the direction of increasing time.

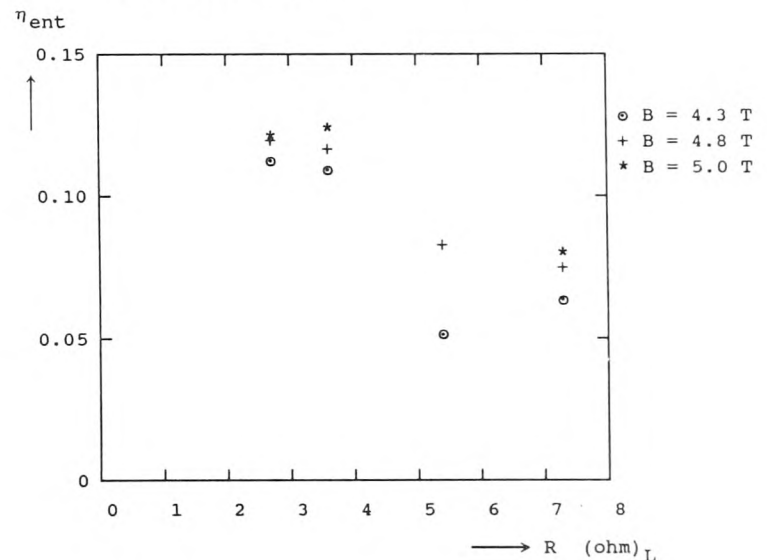


Fig. 10 Enthalpy extraction (η_{ent}) as a function of load resistance (R_L) at $p_s = 7$ bar.

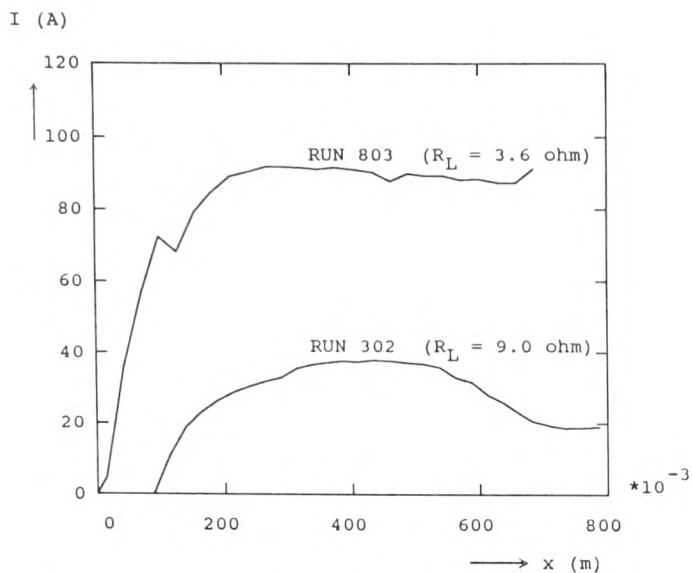


Fig. 11 Current distribution (I) for runs 302 and 803 at maximum power extraction as a function of distance in the generator.

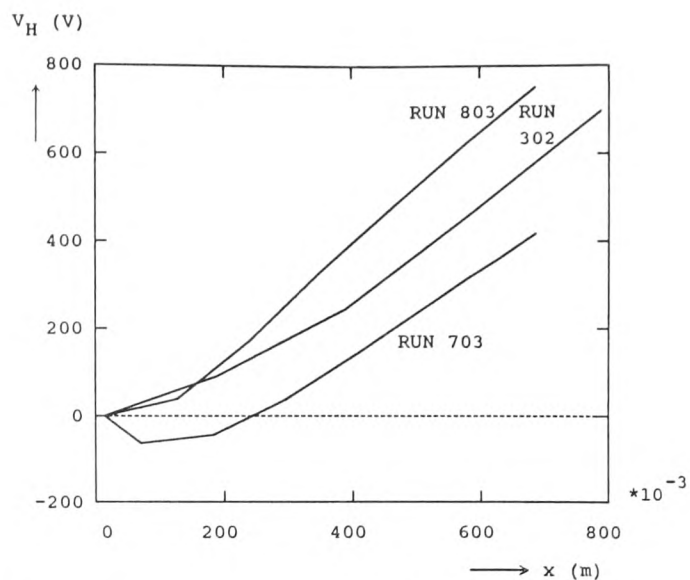


Fig. 12 Hall voltage distribution (V_H) in the generator channel for runs 302, 703 and 803.

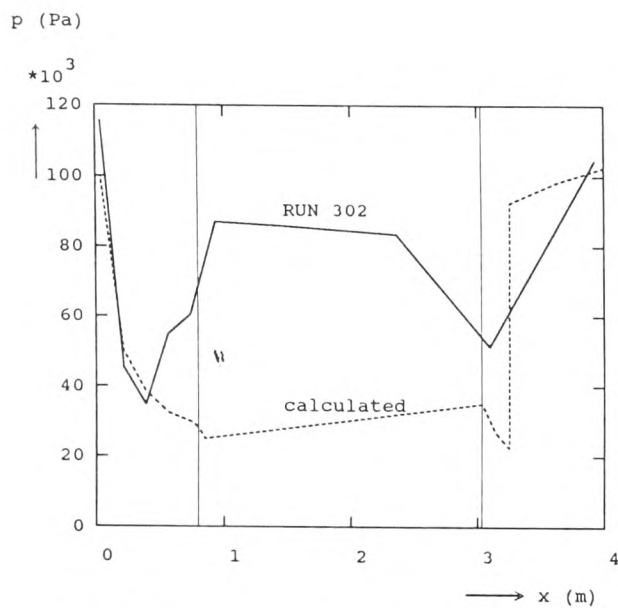


Fig. 13 Static pressure (p) as a function of distance in generator, supersonic diffuser and subsonic diffuser ($P_e = 230$ kW).

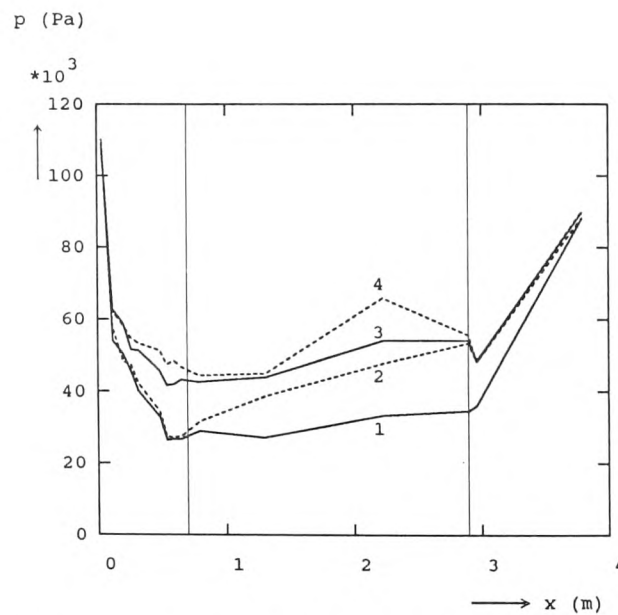


Fig. 14 Static pressure (p) as a function of distance in the hot flow train (generator and diffuser).
 1: run 802, $\eta_{ent} = 8.4\%$ ($B=4.8T$, $R_L=5.4$ ohm),
 2: run 810, $\eta_{ent} = 9.2\%$ ($B=5.4T$, $R_L=7.3$ ohm),
 3: run 803, $\eta_{ent} = 12.9\%$ ($B=5.2T$, $R_L=3.6$ ohm),
 4: run 805, $\eta_{ent} = 12.1\%$ ($B=5.0T$, $R_L=2.7$ ohm).